Supplementary Materials for

IL-6 Blockade Reverses Bone Marrow Failure Induced by Human Acute Myeloid Leukemia

Authors: Tian Yi Zhang[1-3]*, Ritika Dutta[1-3], Brooks Benard[4], Feifei Zhao[1-3], Ravindra Majeti[1-3]

Affiliations:

[1]Department of Medicine, Division of Hematology, Stanford University, Stanford, California, USA.

[2]Stanford School of Medicine, Stanford, California, USA.

[3]Department of Medicine, Division of Hematology, Cancer Institute, and Institute for Stem Cell Biology and Regenerative Medicine, Stanford University, Stanford, California, USA.

[4]Cancer Biology Program, Stanford University School of Medicine, Stanford, California, USA.

*To whom correspondence should be addressed: tzhang8@stanford.edu, rmajeti@stanford.edu

Fig. S1

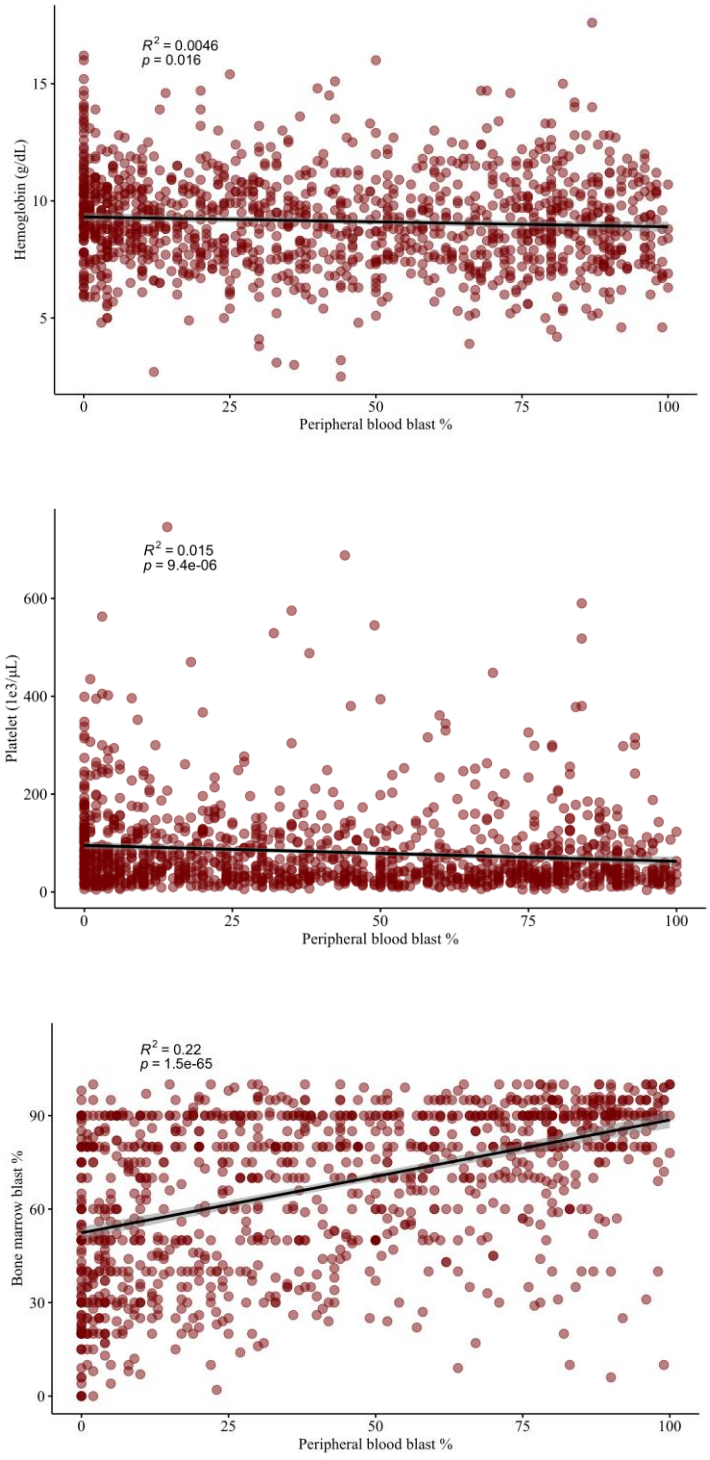
R^2 = 0.0046
p = 0.016
Hemoglobin (g/dL)
15
10
5
0
25
50
75
100
Peripheral blood blast %
R^2 = 0.015
p = 9.4e-06
Platelet (1e3/μL)
600
400
200
0
Peripheral blood blast %
R^2 = 0.22
p = 1.5e-65
Bone marrow blast %
90
60
30
0
Peripheral blood blast %

Peripheral blood leukemic burden does not correlate with cytopenias or BM leukemic burden. (A) hemoglobin (R^2=0.0046, p=0.016), (B) platelet count (R^2=0.015, p=9.4e-06), and (C) PB blast percentage (R^2=0.22, p=1.5e-65) with BM blast percentage at time of diagnosis. R^2=Pearson correlation of determination.

Fig. S2

A.

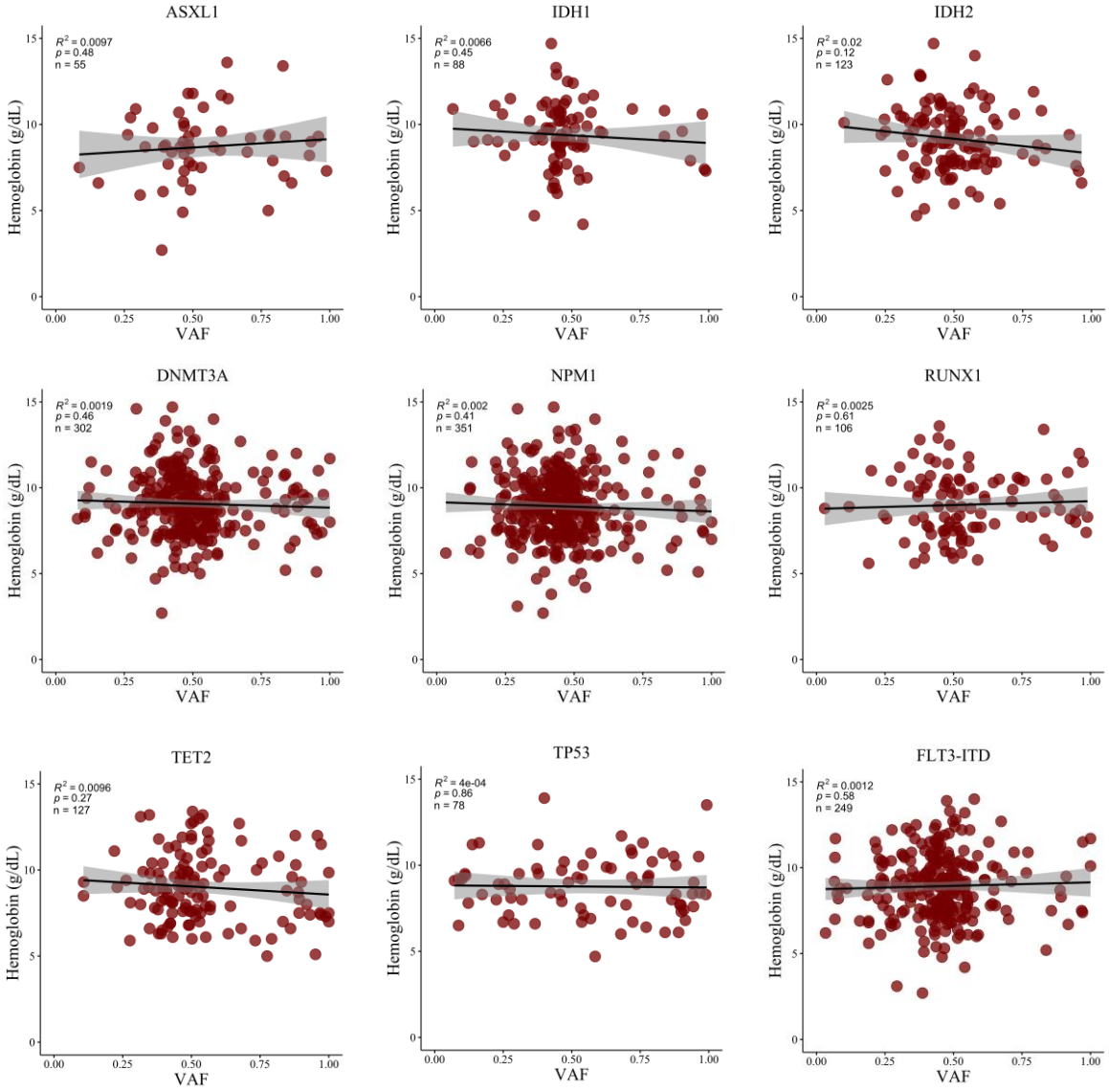
ASXL1
R^2 = 0.0097
p = 0.48
n = 55
IDH1
R^2 = 0.0066
p = 0.45
n = 88
IDH2
R^2 = 0.02
p = 0.12
n = 123
DNMT3A
R^2 = 0.0019
p = 0.46
n = 302
NPM1
R^2 = 0.002
p = 0.41
n = 351
RUNX1
R^2 = 0.0025
p = 0.61
n = 106
TET2
R^2 = 0.0096
p = 0.27
n = 127
TP53
R^2 = 4e-04
p = 0.86
n = 78
FLT3-ITD
R^2 = 0.0012
p = 0.58
n = 249
Hemoglobin (g/dL)
VAF

B.

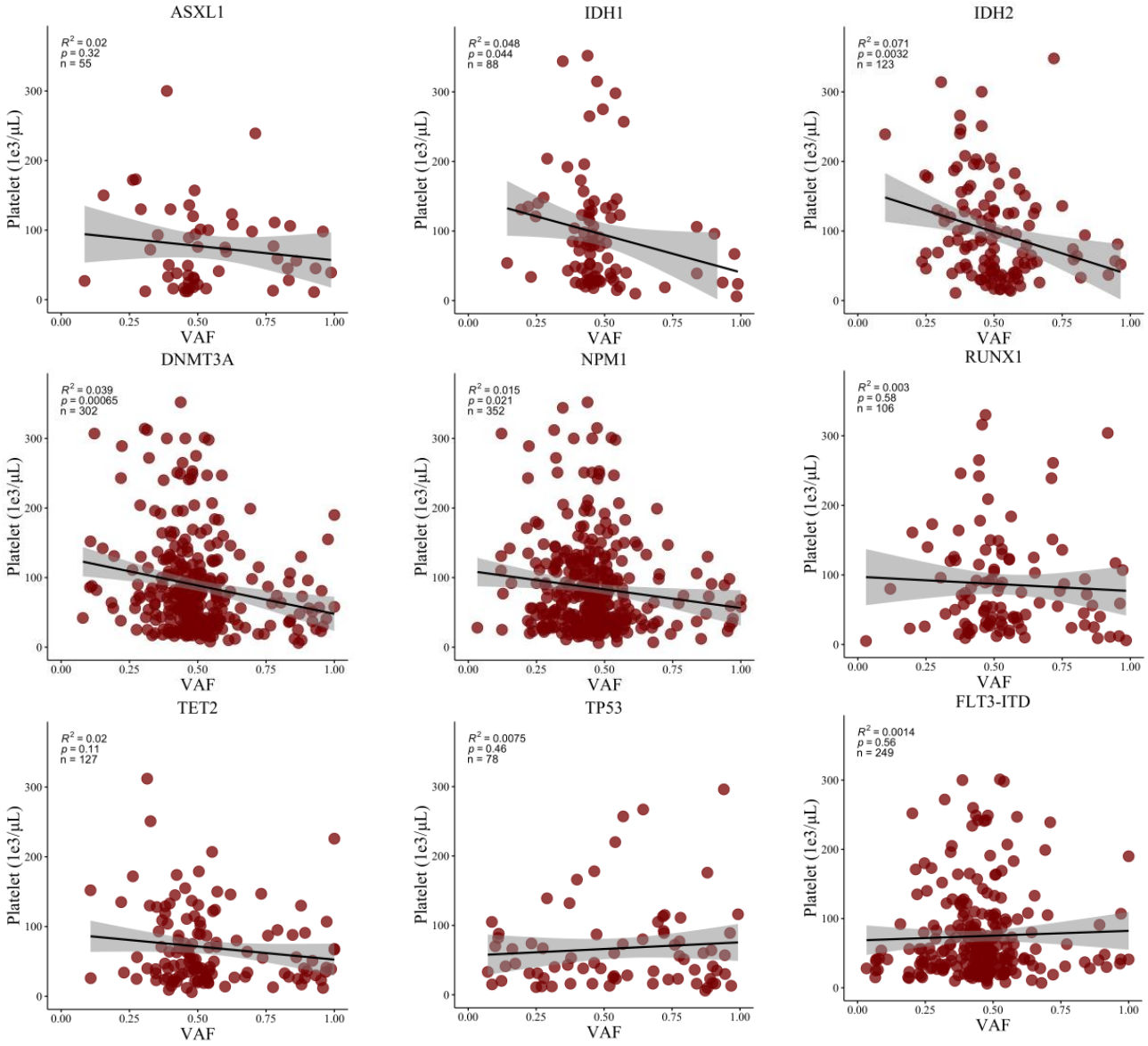

Leukemic burden estimated by variant allelic frequency does not correlate with severity of cytopenias. Correlation of (A) hemoglobin and (B) platelet count with VAF of recurrently mutated genes in AML. R^2=Pearson correlation of determination.

Fig. S3.

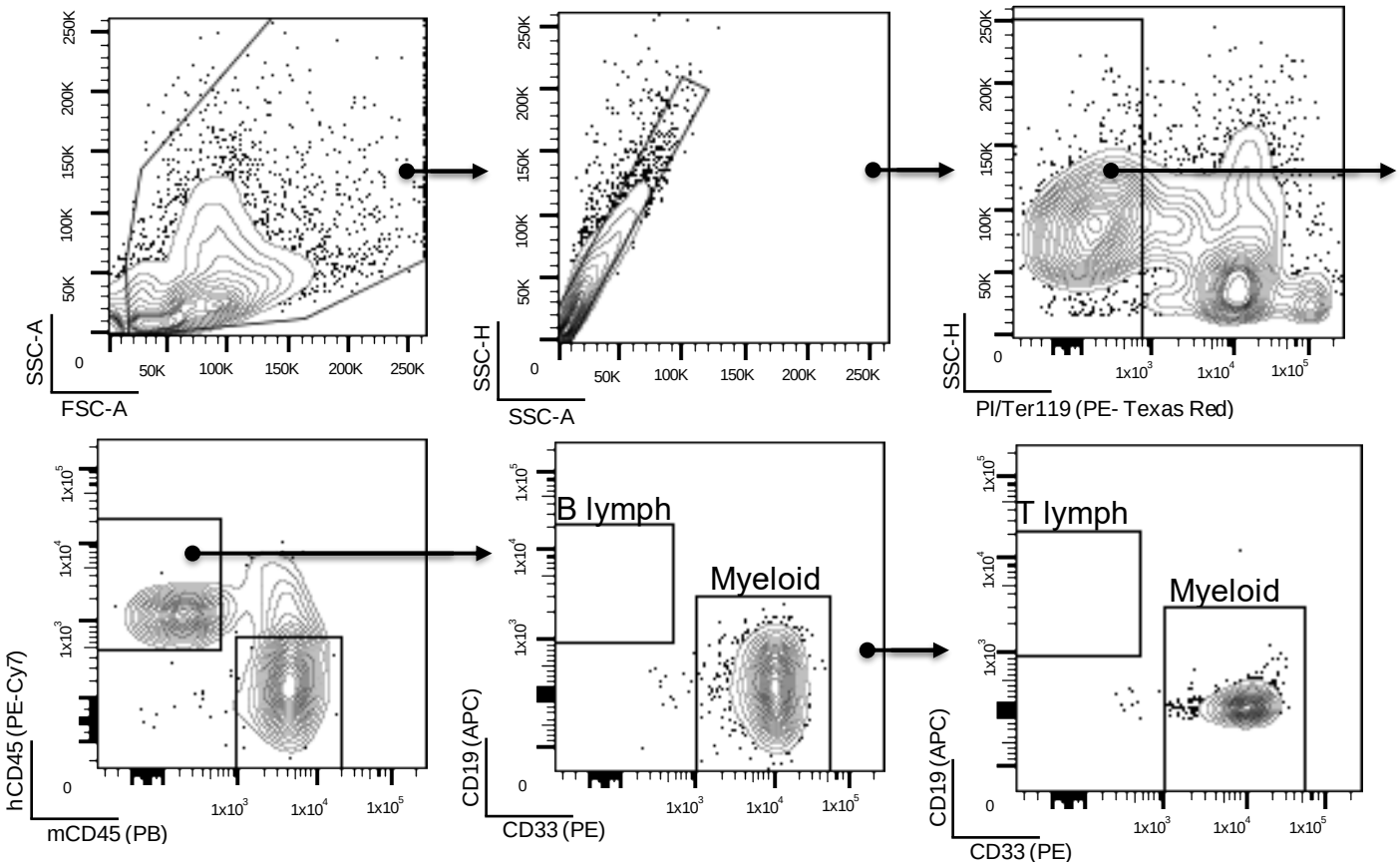

Representative markers and gating strategy to determine human AML engraftment in NSG mice. Femoral aspirates were obtained at 12 weeks after transplantation and stained with a panel of human myeloid- and lymphocyte-specific antibodies followed by flow cytometry analysis. The presence of $mCD45^{-}hCD45^{+}CD33^{+}CD3^{-}CD19^{-}$ cells is indicative of successful engraftment by human AML. Mice with bi-lineage engraftment (with additional presence of $mCD45^{-}hCD45^{+}CD33^{-}CD3^{-}CD19^{+}$ cells) after transplantation would be indicative of engraftment with normal human multipotent progenitors rather than leukemic cells and were therefore excluded from analysis.

Figure. S4.

A.

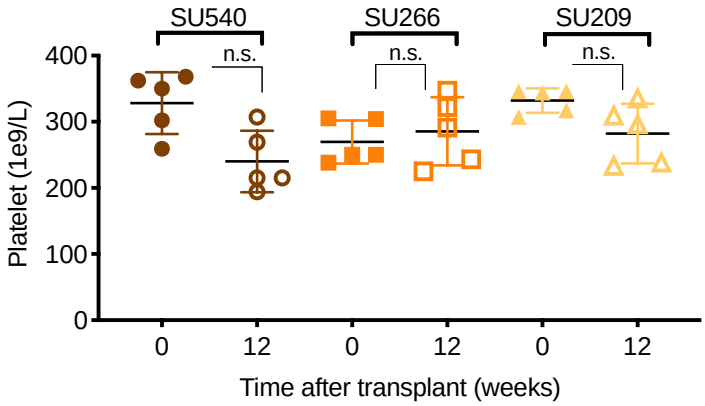

B.

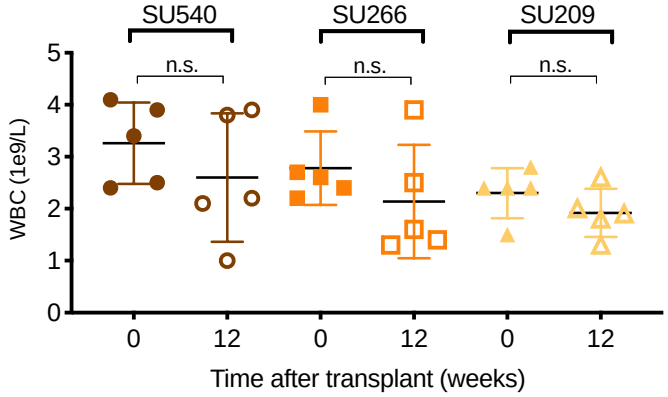

Conventional NSG AML xenografts do not develop BM failure evidenced by lack of cytopenias. (A) Platelet and (B) WBC count was measured via tail vein every two weeks, and results at 12 weeks are shown (n.s. = not significant).

Fig. S5

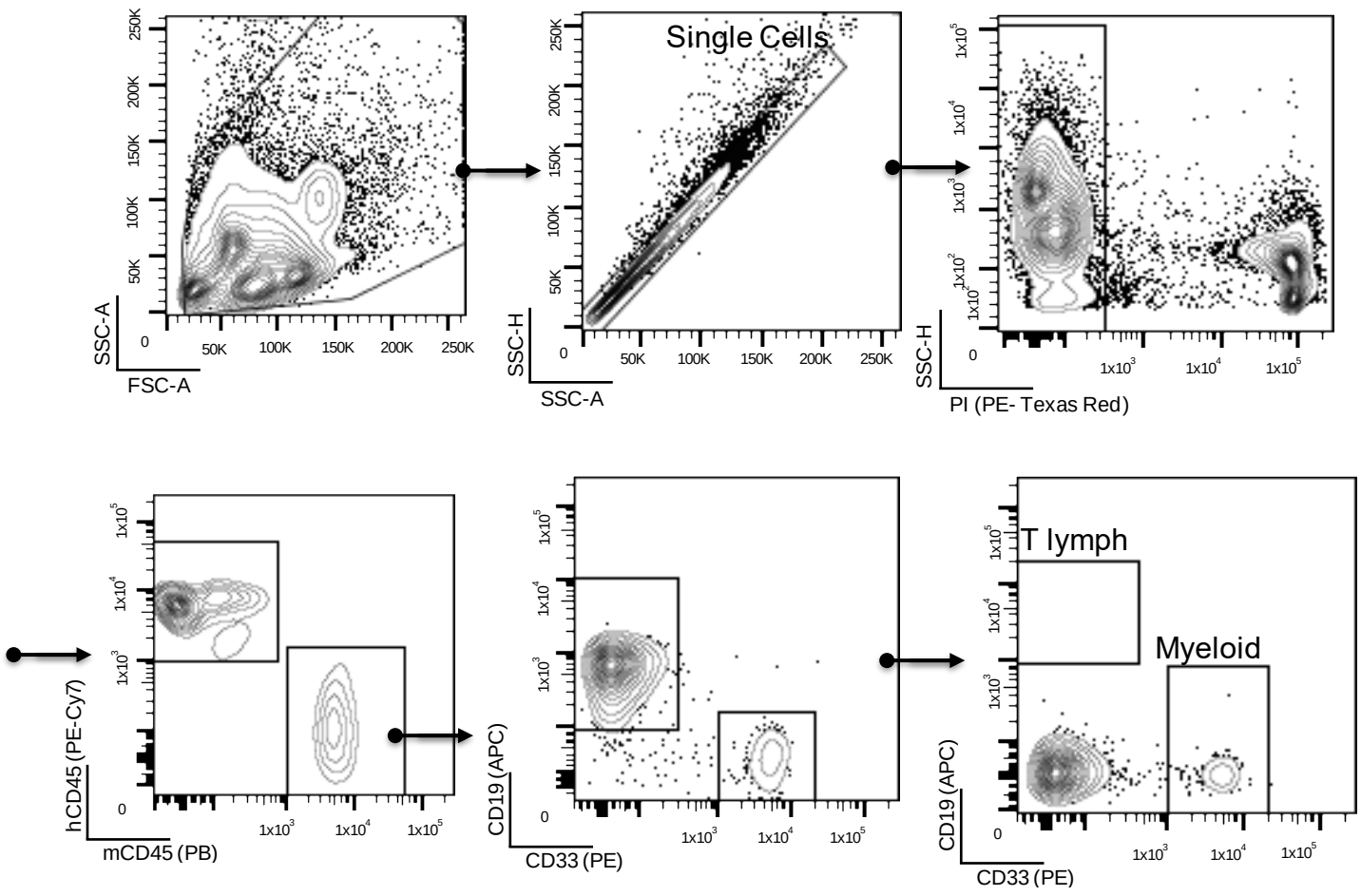

Representative markers and gating strategy to determine human normal CB-CD34$^+$ cell engraftment in NSG mice. Femoral aspirates were obtained at 12 weeks after transplantation and stained with a panel of human myeloid- and lymphocyte-specific antibodies followed by flow cytometry analysis. Bilineage engraftment with mCD45$^-$hCD45$^+$CD33$^+$CD19$^-$ CD3$^-$ and mCD45$^-$ hCD45$^+$CD33$^-$ CD19$^+$CD3$^-$ cells demonstrates successful engraftment by normal CB-CD34$^+$ cells.

Figure. S6

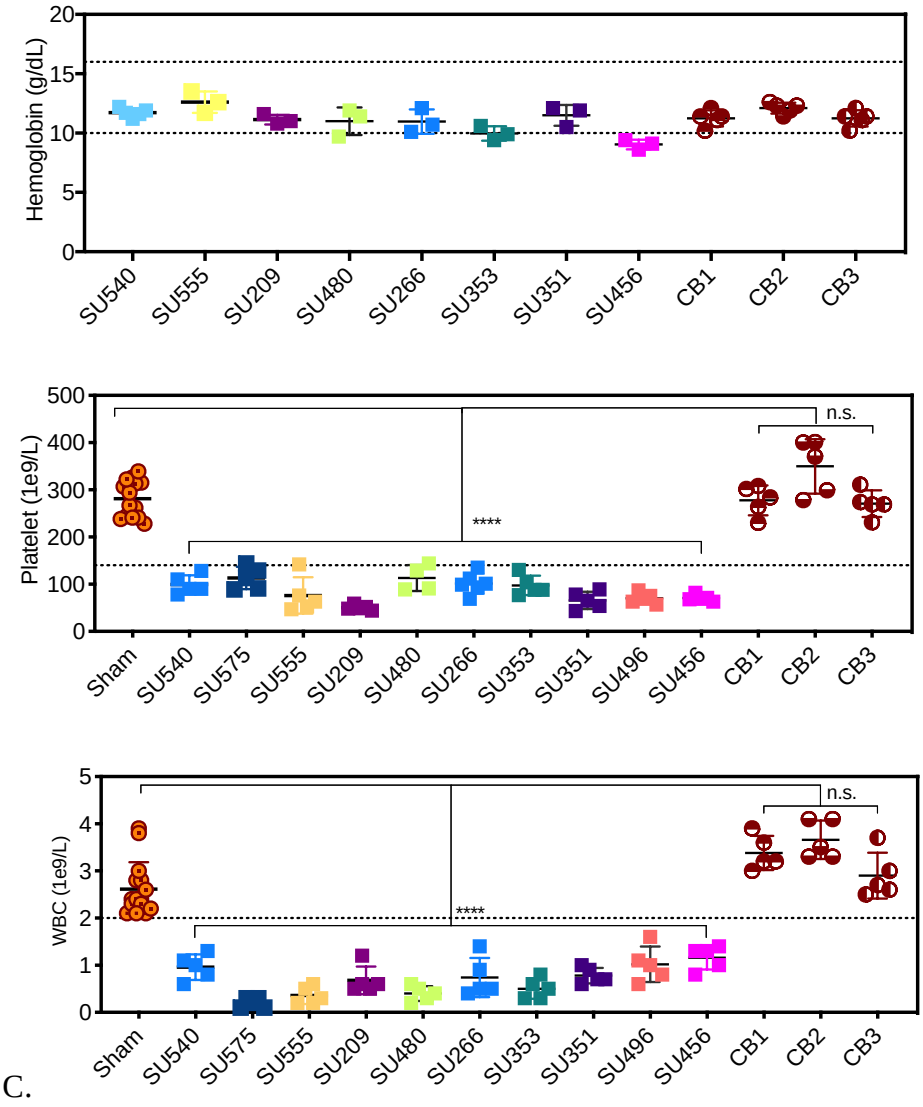

C.

Complete blood counts in NSG^{sham} and NSG^{spln-} mice transplanted with primary AML samples or normal CB-CD34^{+} cells. (A) NSG^{sham} mice engrafted with primary AML or normal CB-CD34^{+} cells do not develop BM failure up to 6 months (8-9 months of age) after transplantation. (B) Thrombocytopenia and (C) leukopenia develop in NSG^{spln-} mice engrafted with AML but not CB-CD34^{+} HSPCs. All AML samples are color coded to reflect individual AML or CB samples reported in Figure 2D.

Fig. S7

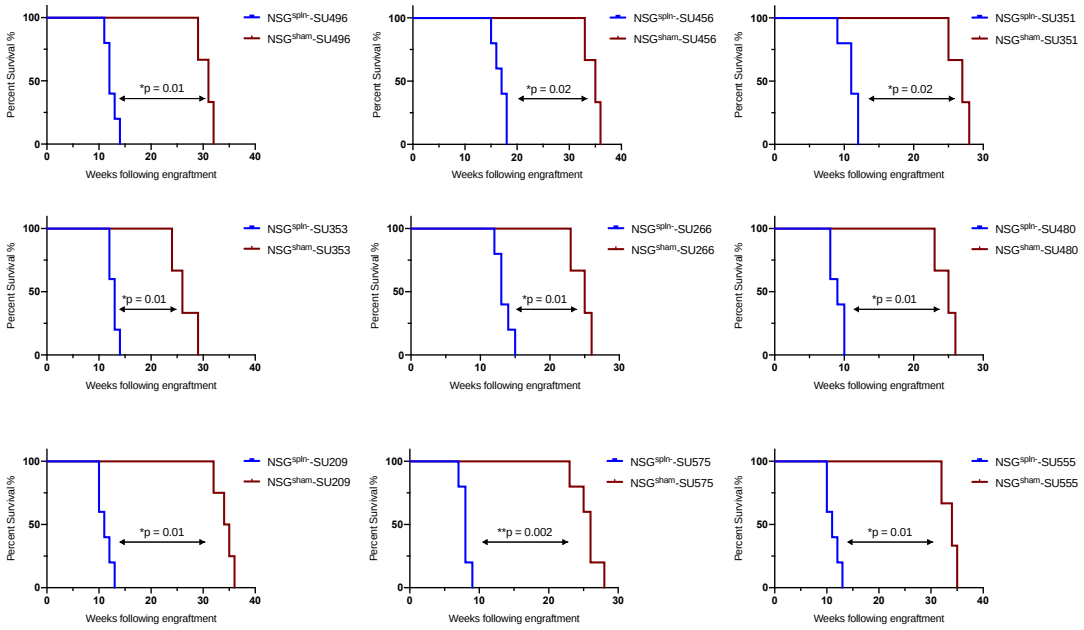

B.

Sample ID	Median Survival (weeks)		P value
	Splenectomized	Sham	
SU540	9.5	36	0.0001
SU575	8	26	0.0002
SU555	11	34	0.01
SU209	11	34	0.009
SU480	9	25	0.01
SU266	13	25	0.01
SU353	13	26	0.01
SU351	11	27	0.02
SU496	12	31	0.01
SU456	17	35	0.02

Splenectomized NSG mice engrafted with human primary AML exhibit shortened survival. (A) Kaplan Meier curves indicating overall survival of NSG^{sham} (n=3-5) and NSG^{spln-} (n=5) mice engrafted with 9 independent primary AML samples as indicated in each plot. (B) Summary of medial survival of each group of NSG^{sham} and NSG^{spln-}. P values were calculated by log-rank test.

Fig. S8

A.

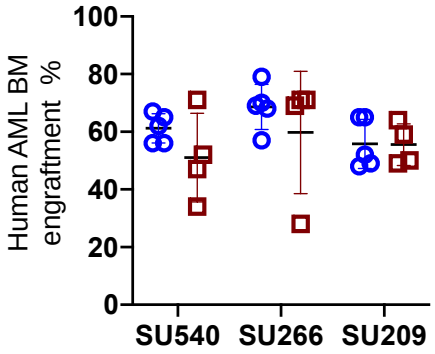
Human AML BM engraftment %
100
80
60
40
20
0
SU540
SU266
SU209

B.

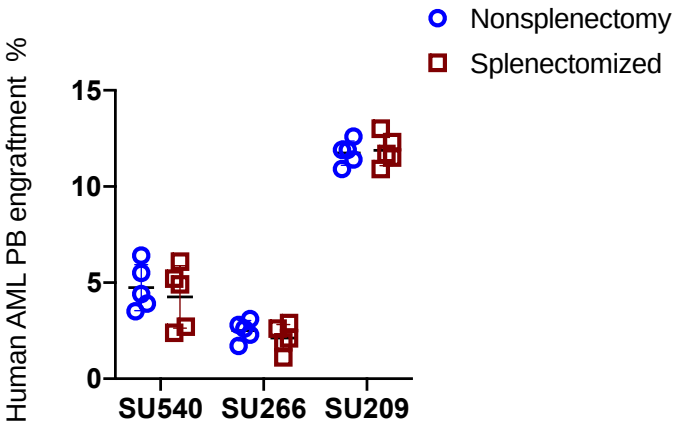
Nonsplenectomy
Splenectomized
Human AML PB engraftment %
15
10
5
0
SU540
SU266
SU209

C.

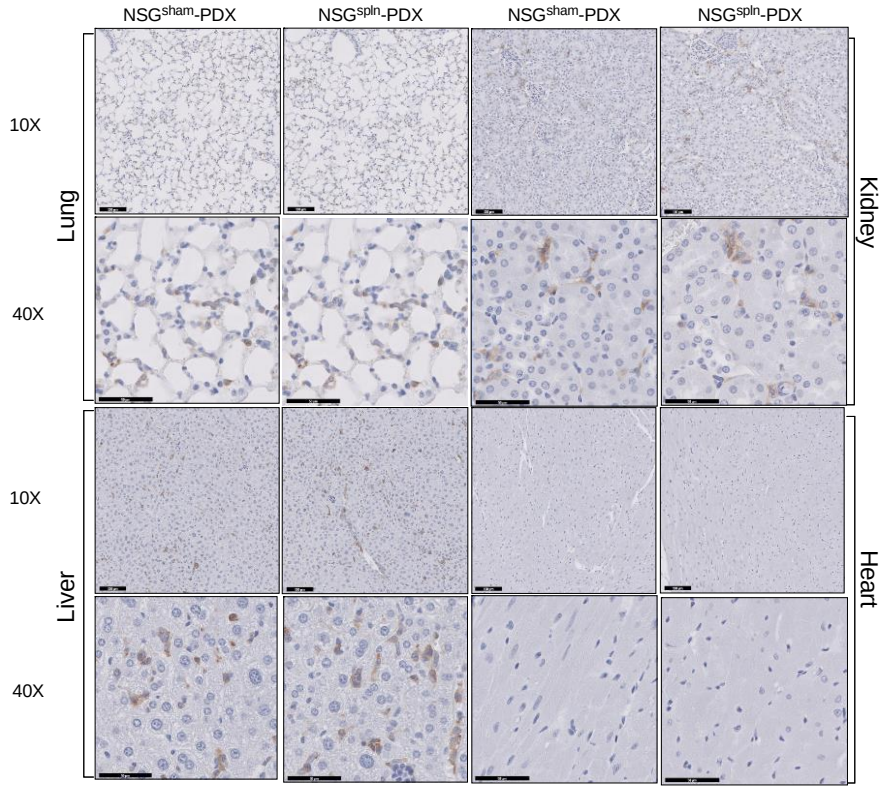
NSGsham-PDX
NSGspln-PDX
NSGsham-PDX
NSGspln-PDX
10X
40X
Lung
Kidney
10X
40X
Liver
Heart

Surgical splenectomy does not increase leukemic burden in NSG mice engrafted with human AML. Human AML disease burden in the (A) BM and (B) PB of NSG^{sham} (n=5) and NSG^{spln-} (n=5) mice engrafted with 3 independent primary AML samples. (C) Representative IHC stain of human CD45 (brown) in the lung, kidney, liver, and heart to estimate organ infiltration of human AML in NSG^{sham} and NSG^{spln-} mice. Scale bars represent 100μm (10x top panel) and 50 μm (40x bottom panel).

Fig. S9

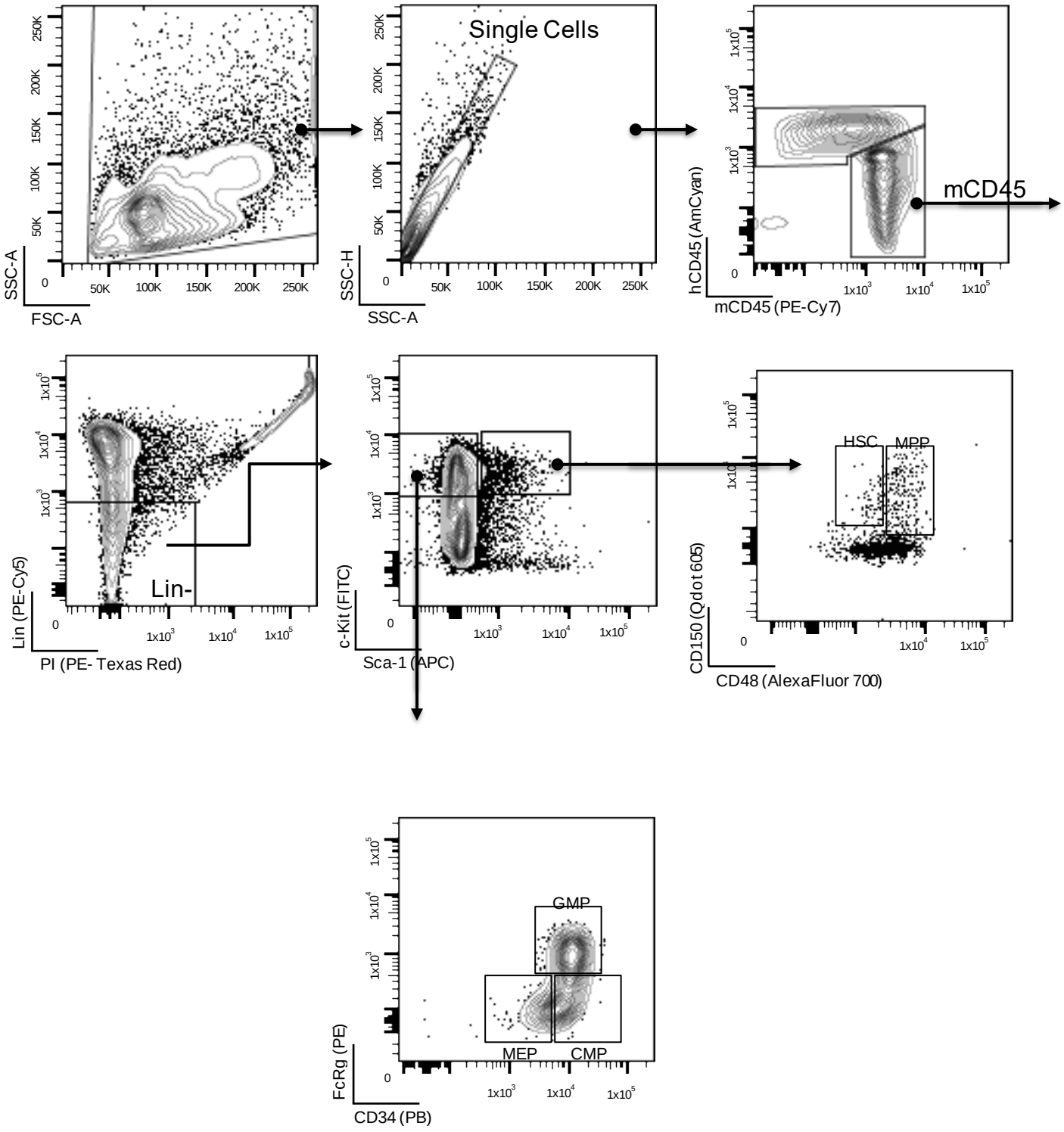
SSC-A
FSC-A
Single Cells
SSC-H
SSC-A
hCD45 (AmCyan)
mCD45 (PE-Cy7)
mCD45
Lin (PE-Cy5)
PI (PE- Texas Red)
Lin-
c-Kit (FITC)
Sca-1 (APC)
HSC
MPP
CD150 (Qdot 605)
CD48 (AlexaFluor 700)
GMP
MEP
CMP
FcRg (PE)
CD34 (PB)

Representative flow plots for the evaluation of mouse hematopoietic stem and progenitor cells in NSG^{spln-}-PDX mice. Splenectomized NSG mice transplanted with human AML blasts or normal human CB-CD34^{+} cells were euthanized at pre-determined time points and mononuclear cell fractions prepared as described. An aliquot of the cells from each mouse was stained with a panel of antibodies designed to evaluate various progenitor populations.

Fig. S10

A.

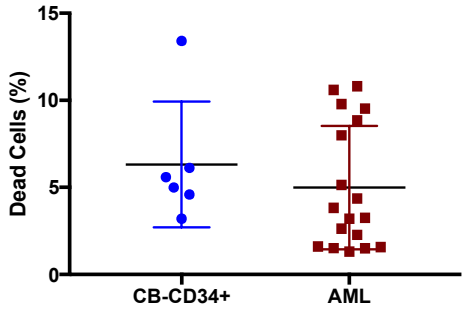

B.

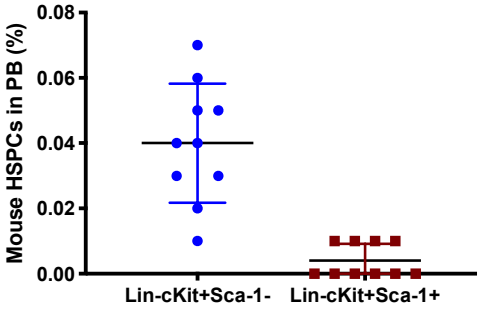

Mouse HSPCs in NSG^{spln-}-PDX mice do not exhibit increased apoptosis/cell death or displacement into PB. (A). The annexin V^+/PI^+ fractions of HSPCs from mononuclear cell fractions of each mouse in Figure 3B-F were used to determine the degree of apoptosis/cell death. (B). The frequency of mouse HSPCs in the PB of NSG^{spln-}-PDX mice was determined at 12 weeks following engraftment.

Fig. S11

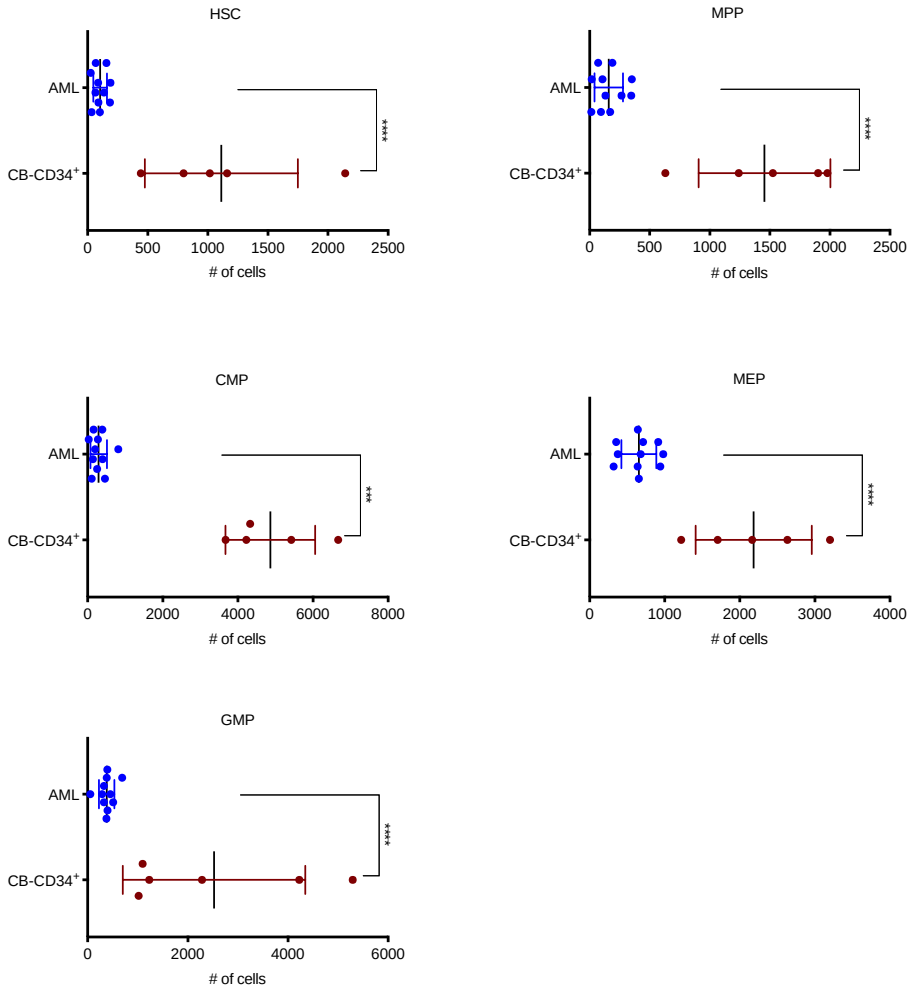

Mouse hematopoietic stem and progenitor cells are similarly depleted in NSG^{sham}-PDX mice. Absolute numbers of HSC (AML 103±25.6 vs CB 1112±185; p<0.0001), MPP (AML 160±37 vs CB 1456±167; p<0.001), CMP (AML 293±35.8 vs CB 4864±358; p<0.0001), MEP (AML 657±35.6 vs CB 2186±247; p<0.0001), and GMP (AML 381±47 vs CB 2525±538; p<0.0012) in NSG^{sham}-PDX (n=5) or NSG^{sham}-CB-CD34^{+} (n=5) mice 8 weeks after transplantation.

Fig. S12

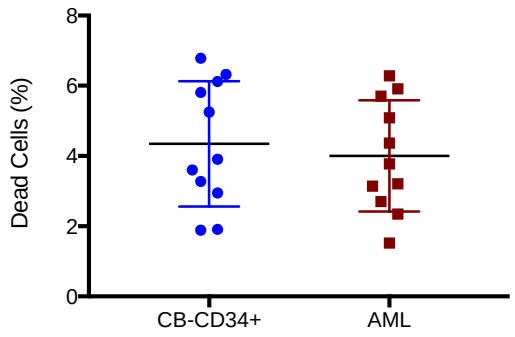

Mouse proerythroblasts in NSG^{spln-}-PDX mice exhibit similar levels of apoptosis/cell death. (A). The percentages of annexin V^+/PI^+ proerythroblasts from each mononuclear cell fractions of each mouse in Figure 3M-P were used to determine the degree of apoptosis/cell death.

Fig. S13.

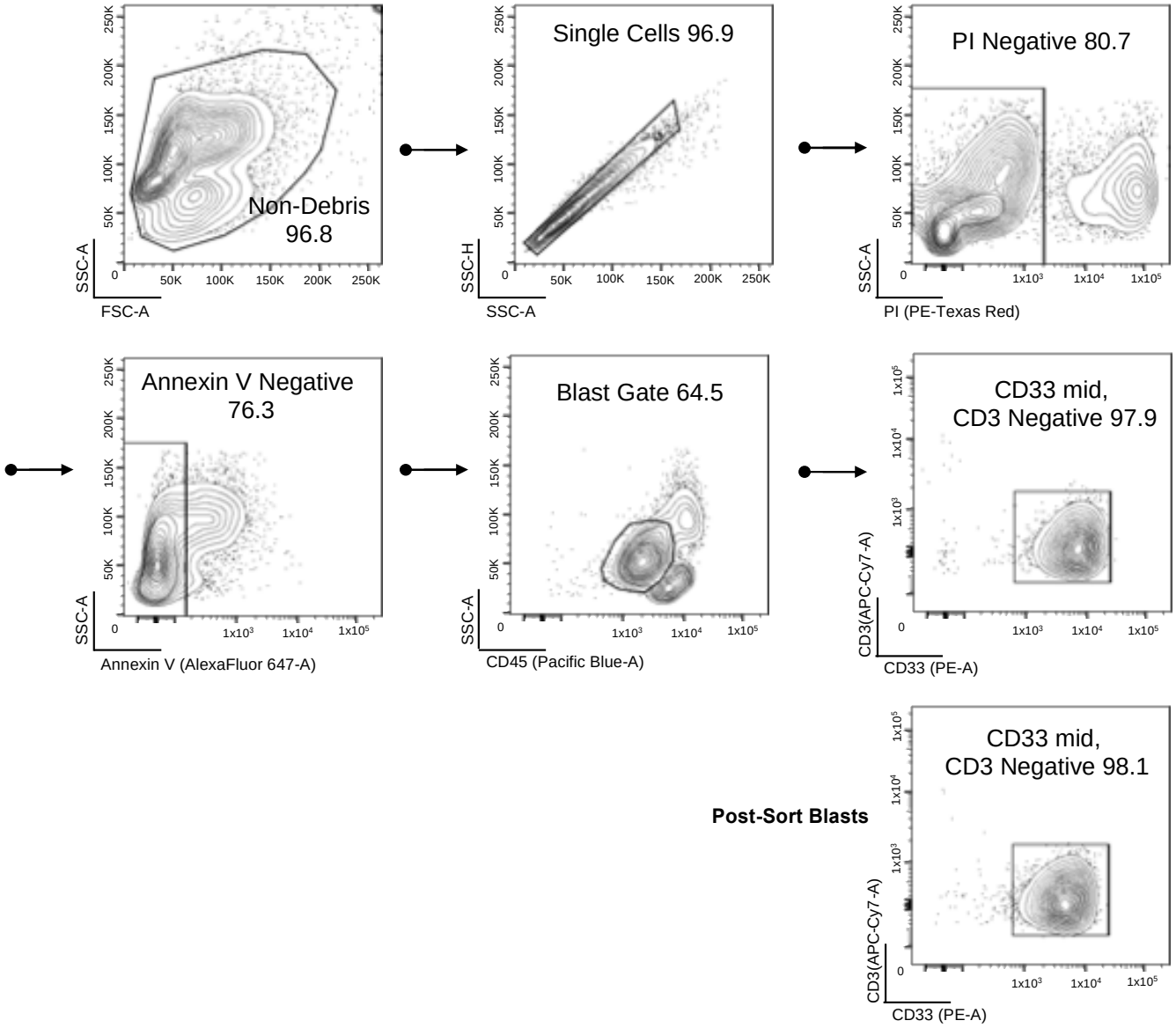

Representative markers and gating strategy used to sort purified populations of human AML blasts. Patient samples were stained to identify human AML blasts expressing $CD45^{mid/low}CD33^{mid}CD3^{-}$. Blast cells were sorted and post-sort analysis was conducted to assess purity.

Fig. S14.

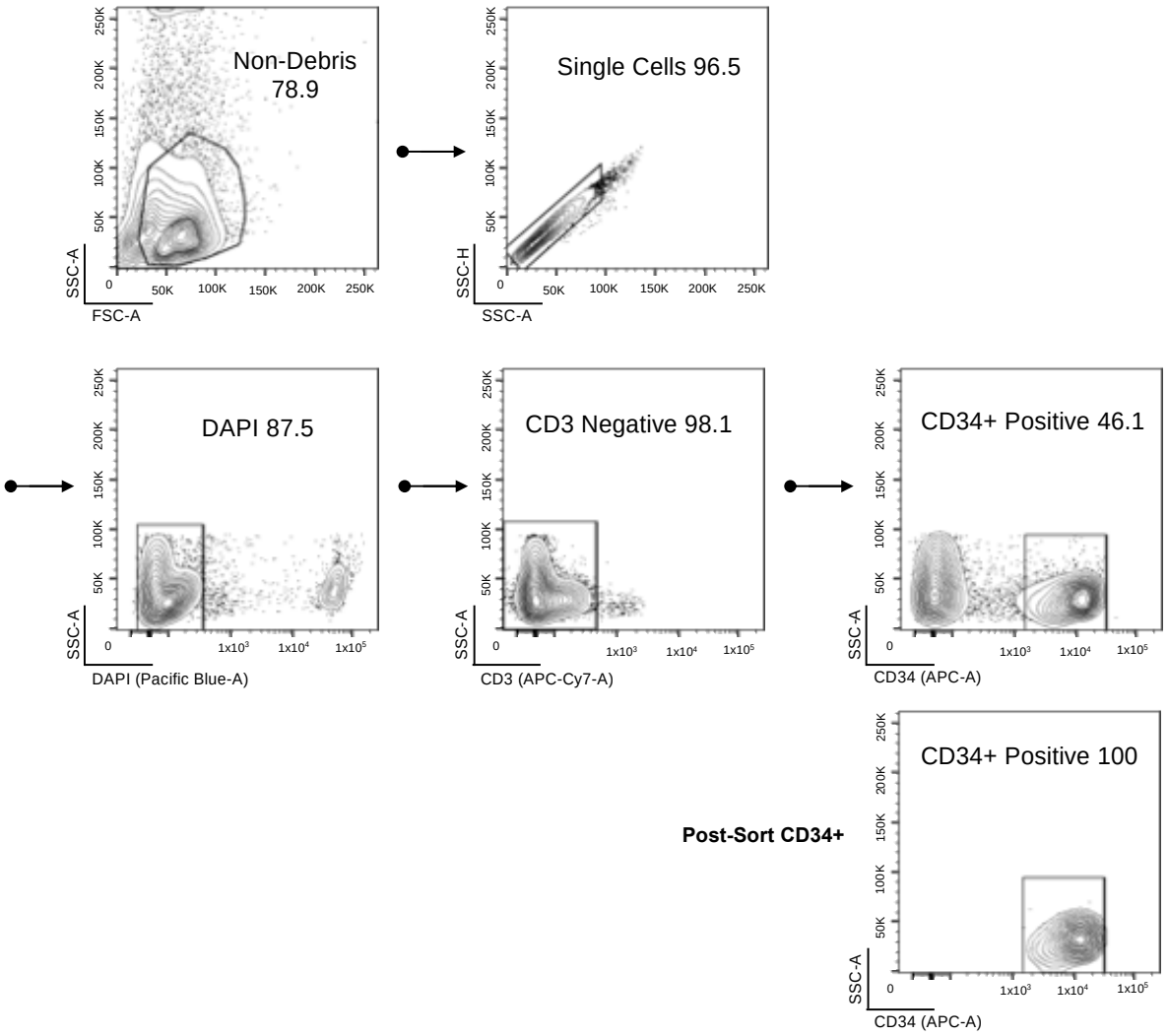

Representative markers and gating strategy used to sort purified populations of human CB-CD34$^+$ cells. Cord blood was enriched for CD34$^+$ cells using positive magnetic selection, and cells were stained using antibodies specific for hCD3 and hCD34 to isolate purified populations of CB-CD34$^+$ progenitors by flow cytometry. A post-sort analysis was conducted to assess purity.

Fig. S15. Viability of primary AML cells.

A.

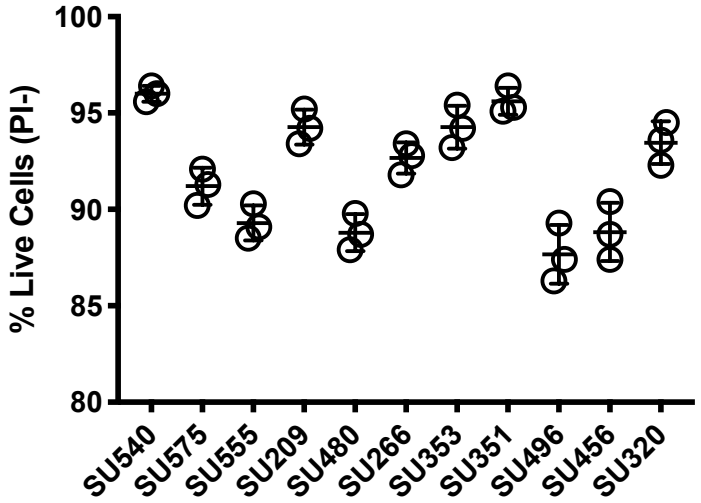

B.

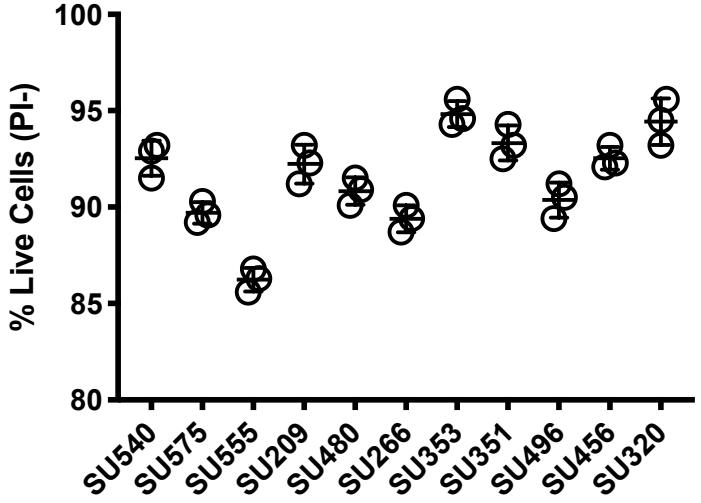

Viability of human AML in culture. (A) Percentages of live (PI^-) human AML cells in culture (14-21 days). (B) Percentages of live (PI^-) human AML blasts flow purified as described at the end of 72 h culture in SFEM supplemented with TPO, SCF, and FLT3L for generation of conditioned medium.

Fig. S16.

A.

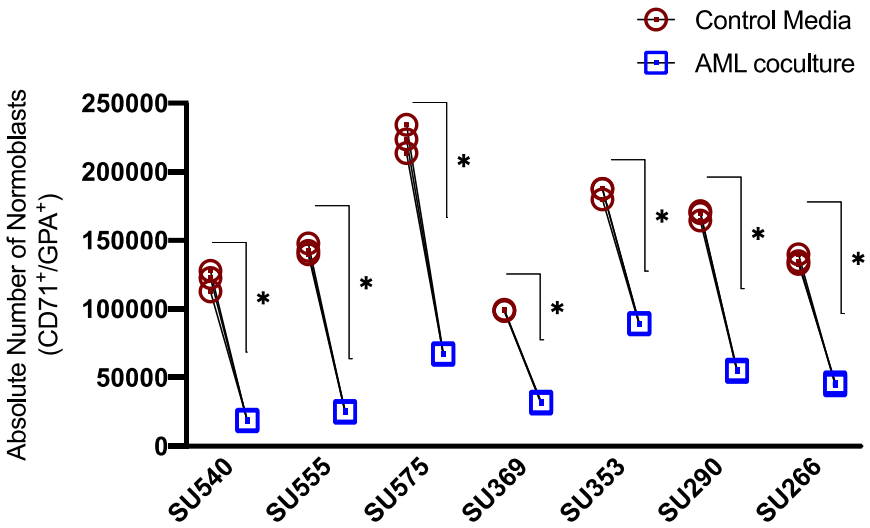
Control Media
AML coculture
Absolute Number of Normoblasts (CD71+/GPA+)
250000
200000
150000
100000
50000
0
*
SU540
SU555
SU575
SU369
SU353
SU290
SU266

B.

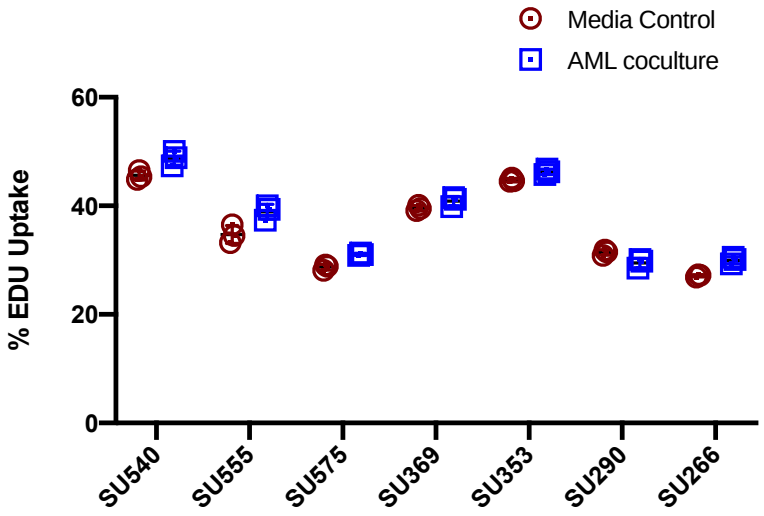
Media Control
AML coculture
% EDU Uptake
60
40
20
0
SU540
SU555
SU575
SU369
SU353
SU290
SU266

C.

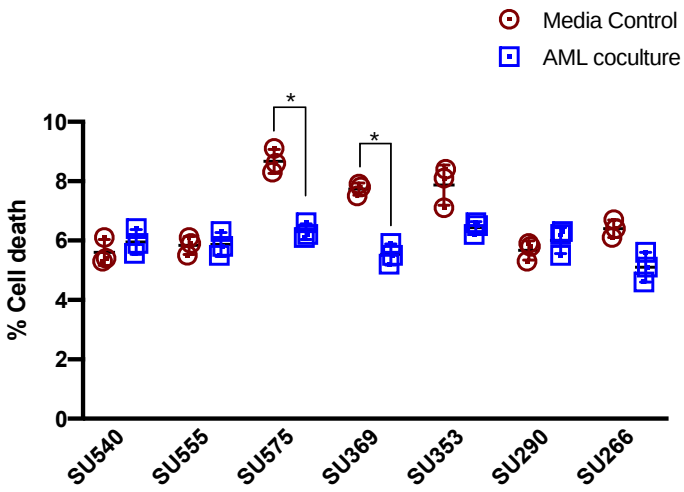

Human AML blasts do not block erythroid differentiation by inhibition of cell cycle entry or induction of cell death. (A) Absolute number of $CD71^+/GPA^+$ normoblasts in culture on day 6 of the transwell assay in the absence or presence of purified AML blasts. *$p<0.01$ by unpaired t-test. (B) Percentage of EDU^+ or (C) PI^+ CB-$CD34^+$ cells in the transwell assay in the absence or presence of purified AML blasts. *$p<0.05$ by unpaired t-test.

Fig. S17.

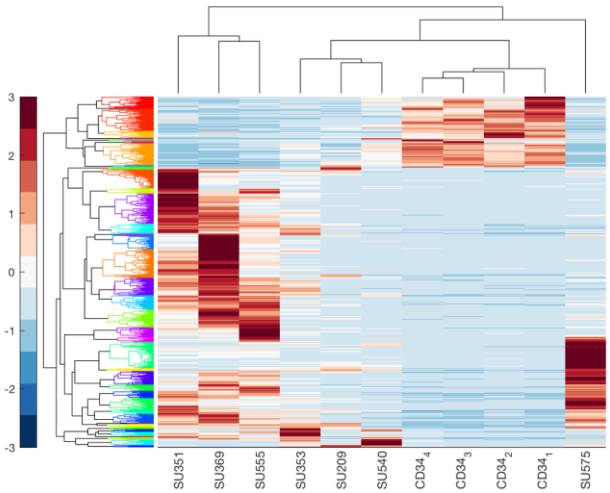

B.

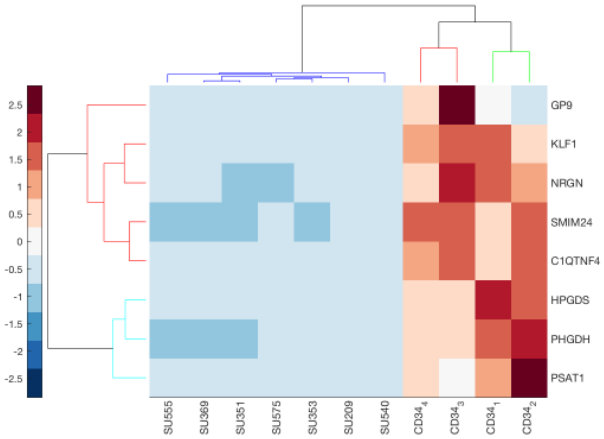

RNA-Seq of purified populations of human AML blasts and CB-CD34$^+$ cells shows an inflammatory transcriptome signature in AML. (A) Heatmap representation of unsupervised hierarchal clustering of the differentially expressed transcripts between purified populations of primary human AML blasts (n=7) and normal CB-CD34$^+$ cells (n=4). (B) Heatmap of the transcripts whose expression was down regulated at least 8 fold ($p < 0.00005$) in AML blasts compared to normal CB-CD34$^+$ cells.

Fig. S18.

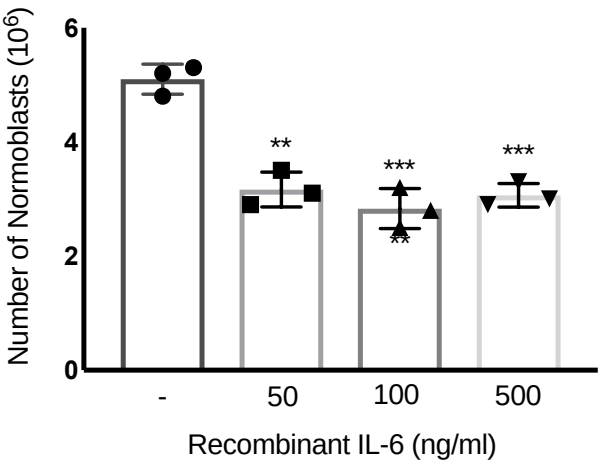

Effects of the addition of recombinant human IL-6 on normal CB-CD34$^+$ progenitors undergoing erythroid differentiation. Recombinant human IL-6 (0-500 ng/ml) was added to triplicate liquid cultures containing normal human CD34$^+$ progenitors (n=3 CB-CD34$^+$ cells from independent donors) in EPO, IL-3, and SCF. The number of CD71$^+$GPA$^+$ cells was determined by flow cytometry on day 6 of culture.

Figure S19

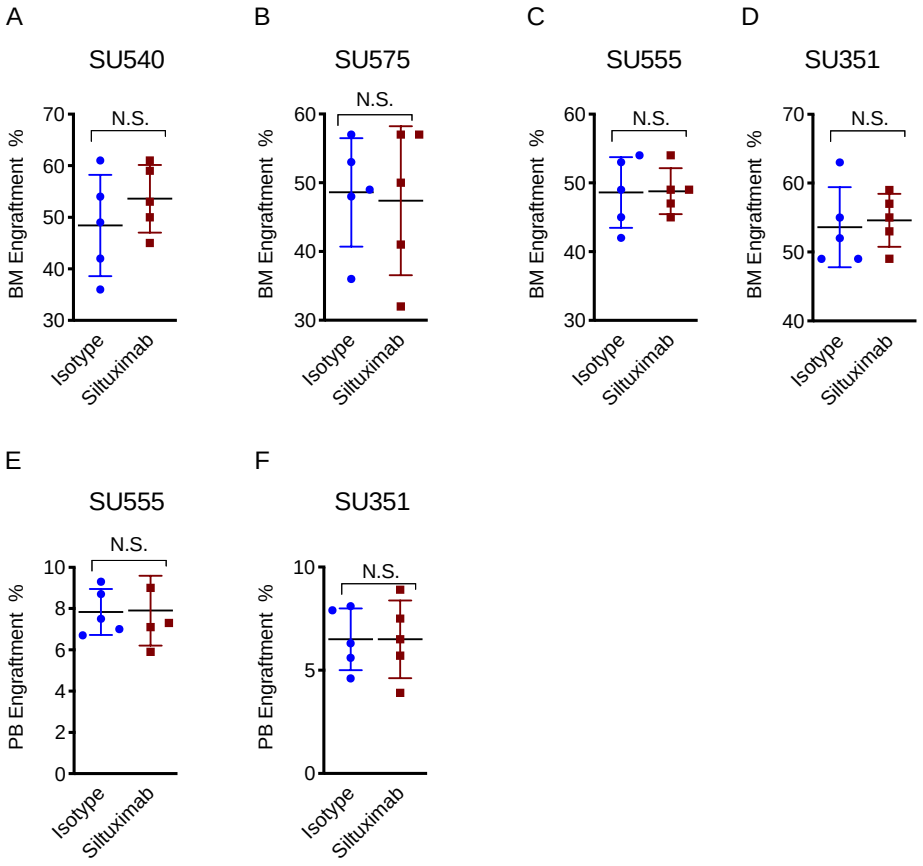

Siltuximab treatment does not decrease leukemic burden in NSG^{spln-} mice engrafted with human AML. NSG^{spln-} mice were engrafted with indicated human AML samples. Control antibody and siltuximab treatment began on day 3 after engraftment and continued every 72 hours until the end of the experiment. Human AML disease burden was examined at week 6-8 in the BM of NSG^{spln-} mice engrafted with (A) SU540, (B) SU575, (C) SU555, (D) SU351. AML burden was assessed in the PB of NSG^{spln-} mice engrafted with (E) SU555 and (F) SU351. N.S. = not significant. N = 5 for all experiments above.

Figure S20

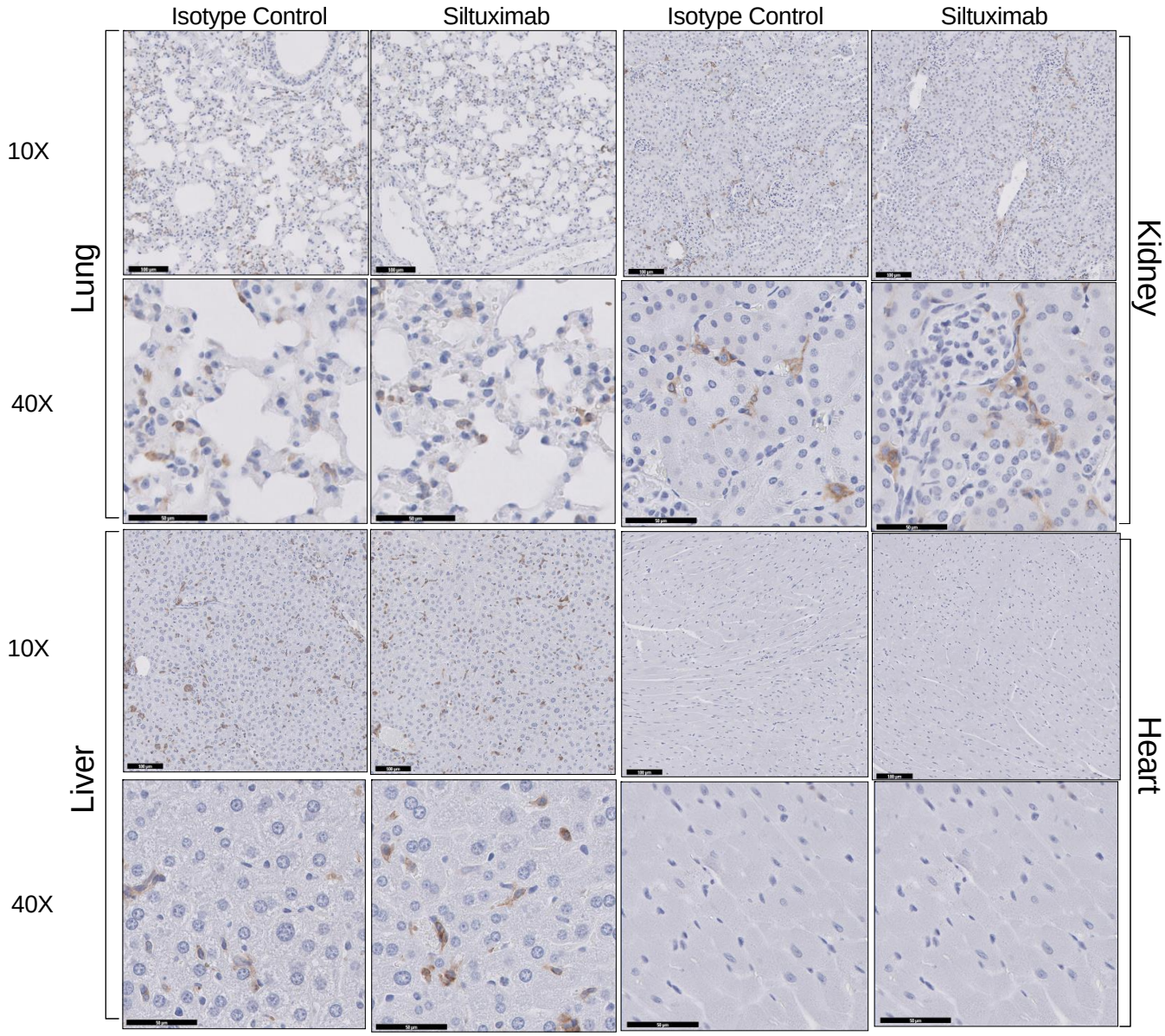

Siltuximab treatment does not decrease leukemic burden in various organs of NSG^{spln-} mice engrafted with human AML. Representative IHC stain of human CD45 (brown) in the lung, kidney, liver, and heart to evaluate organ infiltration by human AML in NSG^{spln-}-PDX (SU540) mice treated with isotype control (n=5) or siltuximab (n=5) as described. Scale bars represent 100µm (10x top panel) and 50 µm (40x bottom panel).

Figure S21

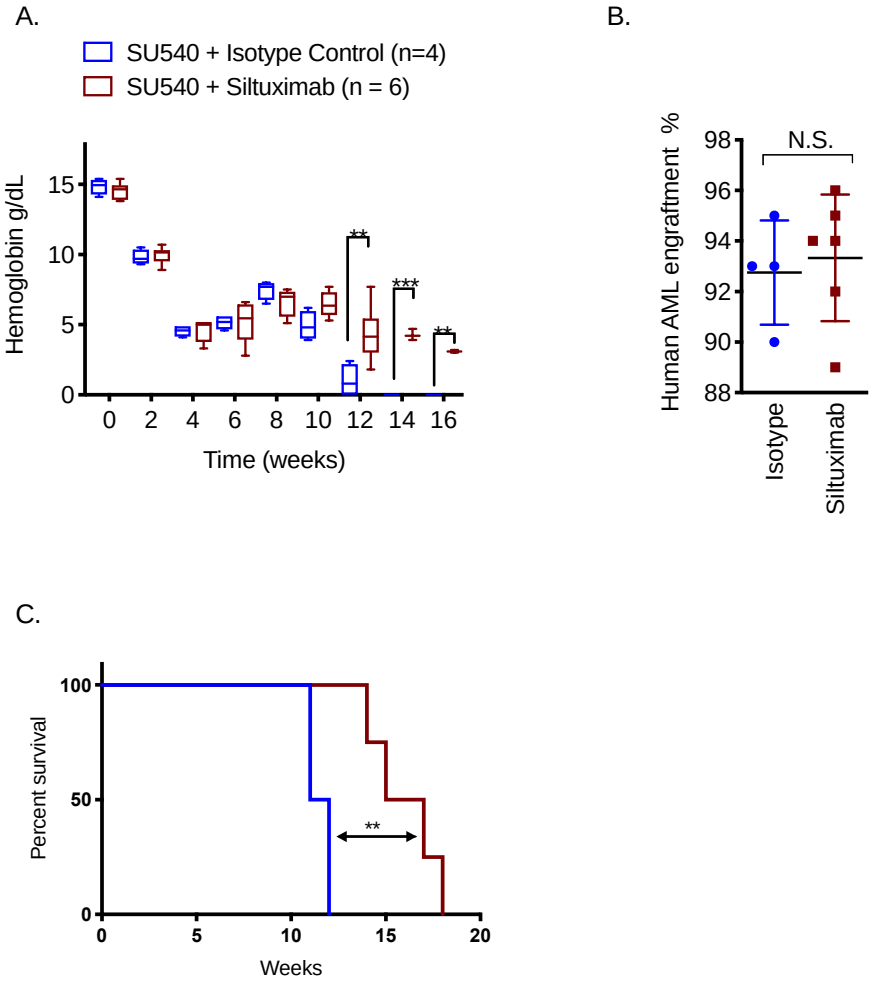

Siltuximab treatment initiated after establishment of disease also improves anemia and overall survival in human AML xenografts. NSG^{spln-}-PDX mice engrafted with SU540 were treated with control antibody or siltuximab (20 mg/kg) every 3 days starting on day 21. (A) The decline in hemoglobin was delayed in the siltuximab treatment group (**p<0.01, ***p<0.001, unpaired t-test). (B) BM leukemic burden (hCD45^{+}CD33^{+}) was similar between treatment groups. N.S.= not significant. (C) Overall survival was improved with siltuximab treatment (11.5 weeks vs 14.5 weeks, **p=0.003, log rank test).

Fig. S22

A.

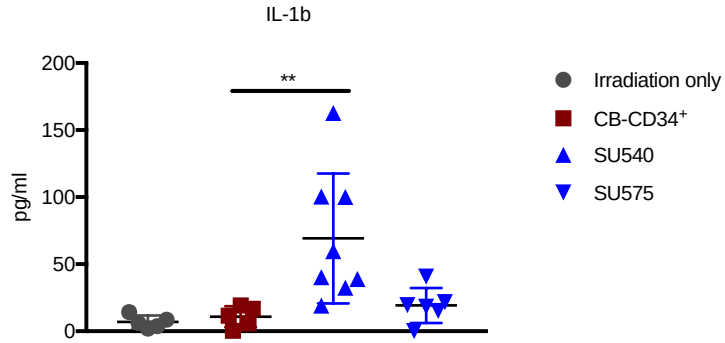

B.

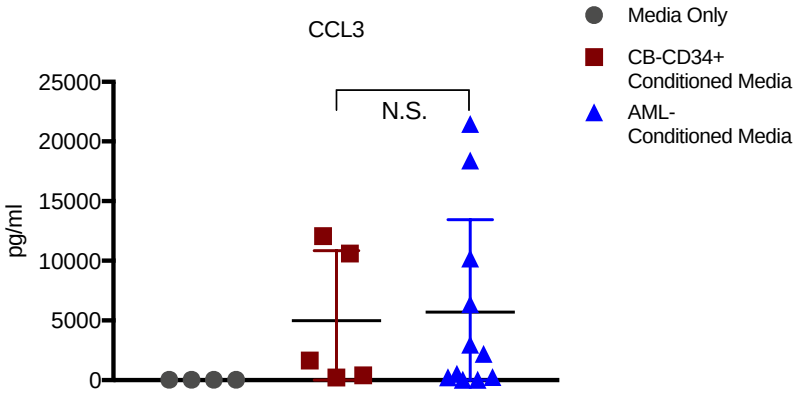

IL-1β and CCL3 production in NSG^{spln-}-PDX mice and AML conditioned medium

(A) IL-1β concentrations in the BM plasma of splenectomized NSG mice engrafted with SU540 and SU575 determined by multiplex protein array (n = 15) compared to similar mice engrafted with CB-CD34$^+$ cells (n=5) or irradiated only control mice (n=4). **p<0.01 unpaired t-test. (B) CCL3 production by purified primary AML blasts (n = 10) in culture determined by multiplex protein array compared to CB-CD34$^+$ cells (n=5) and medium only control (n=4) N.S.=not significant.

Table S1.

Stanford Cancer Center	
Number of Patients	293
Time of Diagnosis	2011-2014
Age (yrs) Mean (SD) Median	 63 (16) 67 (21-89)
Sex Male Female	 169 124
Risk Category (2017 ELN) Favorable Intermediate Adverse	 14 153 126

Summary of patient characteristics whose clinical data were included for analysis in Figure 1A-D ELN: European Leukemia Net risk category

Table S2.

Campbell et al	
Number of Patients	1,376
Time of Diagnosis	2005-2015
Age (yrs) Mean (SD) Median	 47.8 (12.3) 49 (18-84)
Sex Male Female	 740 636
Risk Category (2017 ELN) Favorable Intermediate Adverse	 195 867 204

Summary of patient characteristics whose clinical data were included for analysis in figures S1 and S2. ELN: European Leukemia Net risk category

Figure S3

Sample	Sex	Age	Type	ELN	FAB	CG	Somatic Mutation	WBC	HGB	PLT
SU209	F	66	de novo	INT	M2	46XY	NPM1, FLT3, NOTCH2	166	8.8	133
SU266	M	65	de novo	Adverse	-	Inv(3)	SETD2, TET2, AK2, ASXL1, FLT3-ITD	374	9.9	36
SU351	M	75	secondary MDS-AML	Adverse	M5	Complex	IDH2, NRAS, BCORL1, SETD	3.2	9.7	26
SU353	M	66	de novo	INT	M4	46XY	NPM1, FLT3-ITD, DMNT3A,	111	9.6	73
SU456	M	55	secondary MDS-AML	Adverse	-	Complex	NRAS, TP53	1.8	7.6	146
SU480	F	64	de novo	INT	M1	46XX	CEPBA, FLT3-ITD, DNMT3A, TET2, BCOR, ZRSR2, TET2	16.9	7.4	112
SU496	M	24	de novo	INT	-	(+)8	TP53, IDH2, DNMT3A, STAG2, BCOR, ZRSR2, TET2	35.4	10.3	44
SU540	F	68	de novo	INT	-	46XX	DNMT3A, MYC, CEBPA, NPM1, FLT3-ITD, TET2	94.4	5.6	189
SU555	F	27	de novo	INT	-	-	PTPN11, SETD2, MTND5	103.2	7.5	28
SU575	M	72	secondary MDS-AML	INT	-	46XY	NPM1, FLT3-ITD, DMNT2, ZRSR2, JAK3	28.4	8.3	23

Patient and disease-specific characteristics of human AML samples investigated here.

ELN: European Leukemia Net risk category; FAB: French-American-British AML classification; CG: cytogenetics; WBC: white blood cell (10^3/µl); HGB: hemoglobin (g/dL); PLT: platelet (10^3/µL).

Table S4.

	GM	M	G	GEMM	BFU
Media	14	15	21	23	69
CB-CD34+	21	8	44	22	83
CB-CD34+	20	5	39	21	55
CB-CD34+	10	5	29	14	65
CB-CD34+	15	5	27	16	65
CB-CD34+	16	4	35	19	69
CB-CD34+	17	6	33	19	72
CB-CD34+	13	4	43	20	59
SU540	6	5	36	16	35
SU575	9	12	38	16	37
SU555	10	6	35	17	19
SU209	8	16	33	16	35
SU480	11	14	28	15	32
SU266	11	11	32	15	38
SU353	9	8	27	15	43
SU351	8	11	64	18	37
SU496	9	9	33	17	29
SU456	8	7	31	15	42

Human AML conditioned medium suppresses mouse progenitor colony formation. Number of mouse erythroid and myeloid colonies formed in the presence of control or AML-CM as presented in Figure 4B. All numbers are average values of technical triplicates.

Table S5.

	GM	M	G	GEMM	BFU
Media	14	15	21	23	69
CB-CD34+	21	8	44	22	83
CB-CD34+	20	5	39	21	55
CB-CD34+	10	5	29	14	65
SU540	6	5	36	16	37
SU575	9	12	38	16	37
SU555	10	6	35	17	19
SU209	8	16	33	16	35
SU480	11	14	28	15	38
SU369	11	11	32	15	38
SU456	9	8	27	15	43
SU351	8	11	64	18	37

Human AML-CM suppresses human progenitor colony formation. Number of human erythroid and myeloid colonies formed in the presence of control or AML-CM as presented in Figure 4D. All numbers are average values of technical triplicates.